Procedia Manufacturing
Volume 5, 2016, Pages 621–633
44th Proceedings of the North American Manufacturing Research Institution of SME http://www.sme.org/namrc

A Sensor-Based Method for Diagnostics of Geometric Performance of Machine Tool Linear Axes

Gregory W. Vogl[1], Matthew Calamari[2], Sean Ye[3], and M. Alkan Donmez[1]
[1]National Institute of Standards and Technology (NIST), Gaithersburg, MD, USA
[2]Binghamton University, Binghamton, NY, USA
[3]Northwestern University, Evanston, IL, USA
gvogl@nist.gov, mcalama1@binghamton.edu, seanye2018@u.northwestern.edu, alkan.donmez@nist.gov

Abstract
A linear axis is a vital subsystem of machine tools, and when installed and operating within a manufacturing facility, a machine tool needs to stay in good condition for parts production. All machine tools degrade during operations, yet knowledge of that degradation is elusive; accurate detection of linear axis degradation is a manual and time-consuming process. Thus, manufacturers need automated and efficient methods to diagnose the condition of their machine tool linear axes without disruptions to production. Towards this end, a sensor-based method was developed to quickly estimate the performance degradation of linear axes. The multi-sensor-based method uses data from inclinometers, accelerometers, and rate gyroscopes to identify changes in linear and angular errors due to axis degradation. A linear axis testbed, developed for verification and validation of the sensor-based method, contains a linear axis and a reference laser-based system for measurement of the axis geometric performance. Comparison of the sensor-based results and the laser-based results shows that the sensor-based method is capable of detecting micrometer-level and microradian-level degradation of linear axes. Consequently, if a sensor box resides on a machine tool, then the degradation of the linear axes can be periodically measured and used to help optimize maintenance.

Keywords: Machine tool, Linear Axis, Error, Wear, Degradation, Sensor, Diagnostics, Maintenance

1 Introduction

Linear axes are used to move components of machine tools that carry the cutting tool and workpiece to their desired positions for parts production (Altintas, Verl, Brecher, Uriarte, & Pritschow, 2011). Because a typical machine tool has three linear axes, their positional accuracies directly impact load capacity, quality, and efficiency of manufacturing processes. However, as a machine tool is utilized for parts production, emerging faults lead to performance degradation that lowers control precision and

Selection and peer-review under responsibility of the Scientific Programme Committee of NAMRI/SME

doi:10.1016/j.promfg.2016.08.051

accuracy (Li, Wang, Lin, & Shi, 2014). Typical faults within feed systems are due to pitting, wear, corrosion, cracks, and backlash (Zhou, Mei, Zhang, Jiang, & Sun, 2009). As degradation increases, tool-to-workpiece errors become more likely, and eventually, linear axes of computer numerical controlled (CNC) machines may undergo significant wear that results in a failure and/or a loss of production quality (Uhlmann, Geisert, & Hohwieler, 2008). Faults and failures may become more common as higher levels of manufacturing productivity can result in greater wear on machine components. Machine tool faults account for yearly economic losses of tens of billions of US dollars (Shi, Guo, Song, & Yan, 2012).

Machine tools must be maintained and available for cost-effective production (Verl, Heisel, Walther, & Maier, 2009), yet knowledge of degradation is illusive. While direct methods for machine tool calibration are well-established (International Organization for Standardization, 2012) for position-dependent error quantification, measurements for these methods typically halt production and take "a long time" (Khan & Chen, 2009). The "extensive experimental and analytical efforts" for conventional error measurement methods usually requires expensive equipment, hindering widespread commercial adoption (Ouafi & Barka, 2013). Because degradation differs along a linear axis and the wear changes with production time (Uhlmann et al., 2008), the particular condition of an axis is usually unknown.

Manufacturers need automated and efficient methods for continual diagnosis of the condition of machine tool linear axes without disruptions to production. Efforts to monitor the condition of linear axes components have utilized various sensors:

- Built-in linear and motor encoders (Plapper & Weck, 2001; Zhou, Tao, Mei, Jiang, & Sun, 2011; Zhou, Xu, Liu, & Zhang, 2014) with laser interferometer (Verl et al., 2009)
- Motor torque via current sensors (Li et al., 2014; Uhlmann et al., 2008; Zhou et al., 2009), accelerometers (Feng & Pan, 2012; Huang et al., 2010; Liao & Lee, 2009)
- Accelerometers, thermocouples, and analog controller outputs (torque, speed, and encoder position) (Liao & Pavel, 2012)
- Hall effect sensors (Garinei & Marsili, 2012)
- Piezoresistive thin films (Biehl, Staufenbiel, Recknagel, Denkena, & Bertram, 2012; Möhring & Bertram, 2012)
- Piezoelectric ceramics (Ehrmann & Herder, 2013).

These attempts at condition monitoring of linear axes were limited in success, largely because both external sensors and built-in sensors have limitations. Built-in position sensors are usually highly accurate (Zhou et al., 2011), yet controller signals have problems such as low sample rate, limited sensitivity due to sensors being far from monitored components, and unwanted influences from multiple sources (Plapper & Weck, 2001). On the other hand, external sensors can be more direct and physically sensitive, but high costs and required bandwidths have impeded their application for online monitoring of linear axes (Zhou et al., 2009).

In this paper, a new sensor-based method for diagnostics of machine tool linear axes is presented. The sensor-based method was developed to quickly estimate the performance degradation of linear axes, based on the use of external sensors for high-bandwidth measurements of changes in translational and angular errors of linear axes. The sensors are contained within a sensor box for ease of installation and periodic use on a machine tool, resulting in data collection and analysis with minimal disruption to production. The diagnostics and prognostics of the linear axes can be used to help optimize maintenance and production schedules. The cost-effective sensors are expected to be an overall net positive when factoring in the expected savings in production losses and scrapped parts for a machine tool.

2 Sensor Box Concept for Geometric Performance Assessment

The goal of the new sensor-based method is to enable efficient monitoring of the change in positioning errors, and hence the change in tool-to-workpiece positioning performance, due to degradation of linear axes. This section outlines these errors, the concept of the sensor-based methodology, and the needed uncertainties of the method.

2.1 Straightness and Angular Errors

Even without degradation, the carriage of a linear axis translates and rotates due to imperfections as the carriage moves along the guideways of the linear axis. Figure 1 shows these six errors that change with axis degradation. As the carriage is positioned along the X axis, it encounters three translational errors from its nominal path: one linear displacement error (E_{XX}) in the X-axis direction and two straightness errors (E_{YX} and E_{ZX}) in the Y- and Z-axis directions. The carriage also experiences three angular errors (E_{AX}, E_{BX}, and E_{CX}) about the X-, Y-, and Z-axes.

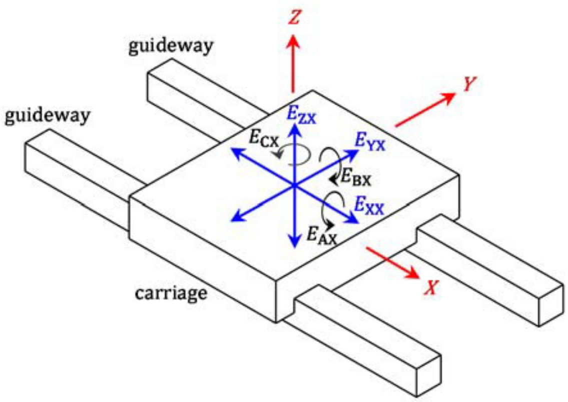

Figure 1. Translational and angular errors of a component commanded to move along a (nominal) straight-line trajectory parallel to the X-axis.

A typical machine tool has three linear axes, which means that a total of 18 (= 6 × 3) translational and angular errors exist. These errors are major contributors to the position-dependent tool-to-workpiece errors.

2.2 Sensor Box Concept

Sensors can be used to measure changes in the straightness and angular errors due to degradation. Figure 2 shows a sensor box on a typical 3-axis machine tool with 'stacked' linear axes; the Z axis is on the X axis, which is on the Y axis. The sensor box is attached to the Z-axis slide, so that if any axis is moved, the sensor box moves and will detect motion. Accelerometers are used to detect translational errors, and inclinometers and rate gyroscopes are used to detect angular errors. For the machine tool configuration shown in Figure 2, changes in the positioning errors could be estimated by using the data from the sensor box and the box's position relative to the tool tip. Therefore, the sensor box is focused on tracking the effects of degradation of each linear axis on the machining performance.

Degradation may be tracked periodically by data collection during a fixed-cycle test (Garinei & Marsili, 2012; Huang et al., 2010; Liao & Lee, 2009; Verl et al., 2009; Zhou et al., 2009; Zhou et al., 2011), in which the machine tool axes are commanded to move via the same program (the fixed cycle) with the machine tool initially in the same state (temperature, etc.). The collected data is then processed and compared to the previous results to determine the degradation from one test to another.

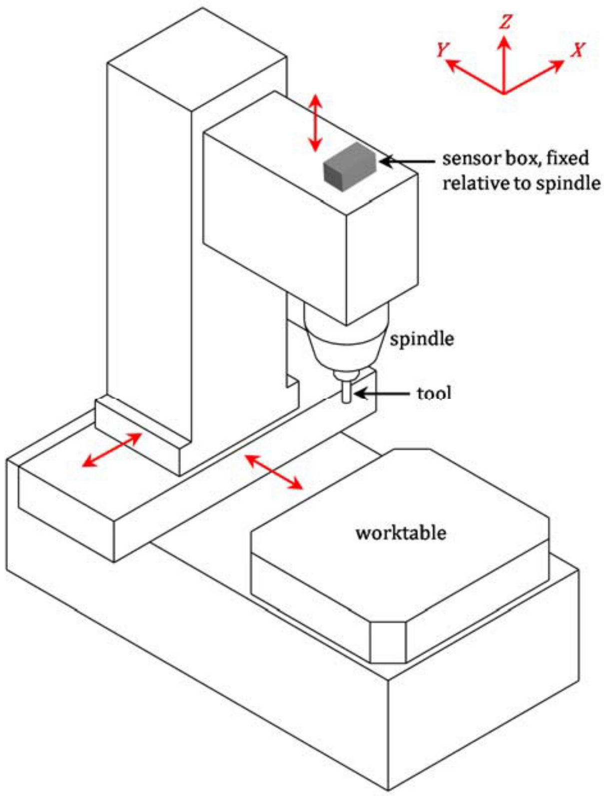

Figure 2. Schematic of sensor box on machine tool for metrology of linear axis degradation.

Table 1 outlines some properties of the sensors used for the fixed-cycle tests. The reason for two types of angular sensors is that the inclinometer may measure low-frequency angular error terms with greater accuracy than the rate gyroscope. Details of the fixed-cycle test and data processing for the determination of error changes will be described in later sections.

Table 1. Properties of sensors used in sensor box.

Sensor	Bandwidth[a]	Noise
Accelerometer	0.02 Hz to 1700 Hz	2.9 $(\mu m/s^2)/\sqrt{Hz}$ at 1 Hz to 0.4 $(\mu m/s^2)/\sqrt{Hz}$ at 1 kHz
Inclinometer	0 Hz to 2 Hz	2.4 μrad[b]
Rate gyroscope	0 Hz to 200 Hz	0.002 $°/s/\sqrt{Hz}$

[a] frequencies correspond to half-power points, also known as 3 dB points

[b] maximum deviation at 0 Hz

2.3 Tolerances for Errors

The sensor-based method depends on the available sensors, whose selection depends on the magnitude of errors to be detected and the accuracy with which they need to be identified. Small levels of degradation of linear axes are expected and allowed, but there are limits specified for axis errors. ISO 10791-2 (International Organization for Standardization, 2001) specifies the tolerances for linear axis errors of vertical machining centers. As shown in Table 2, the acceptable straightness error is limited to 20 μm and the acceptable angular error is limited to 60 μrad.

Table 2. Tolerances for linear axis errors of vertical machining centers.

Error	Tolerance*
Straightness	20 μm
Angular (Pitch, Yaw, or Roll)	60 μrad

* for axes capable of 1 meter of travel, according to ISO 10791-2 (International Organization for Standardization, 2001)

The measurement uncertainties must be less than the respective specified tolerances to measure the errors. The test uncertainty ratio (TUR), which is the ratio of the tolerance to the uncertainty of the measurement, should be sufficiently large. Typically, a TUR of at least 4:1 is recommended; the larger, the better for a measurement system. We will accept a TUR of at least 4:1 based on design constraints such as sensor cost and size. Thus, we will accept straightness and angular error measurement uncertainties of 5 μm and 15 μrad, respectively, based on the tolerances outlined in Table 2.

3 Sensor-Based Method

A sensor-based method was developed to satisfy the TUR constraint of 4:1. This section summarizes the sensor box, the fixed-cycle test, and the sensor-based methodology for determination of changes in straightness and angular errors.

3.1 Sensor Box

Figure 3 presents a photorealistic picture (sans cables and top) of the sensor box, which is composed of two inclinometers, one tri-axial rate gyroscope (three rate gyroscopes), and three accelerometers. Each sensor detects a component of the translational or angular errors seen in Figure 1. The relationships of the sensors to these error components are noted in Figure 3.

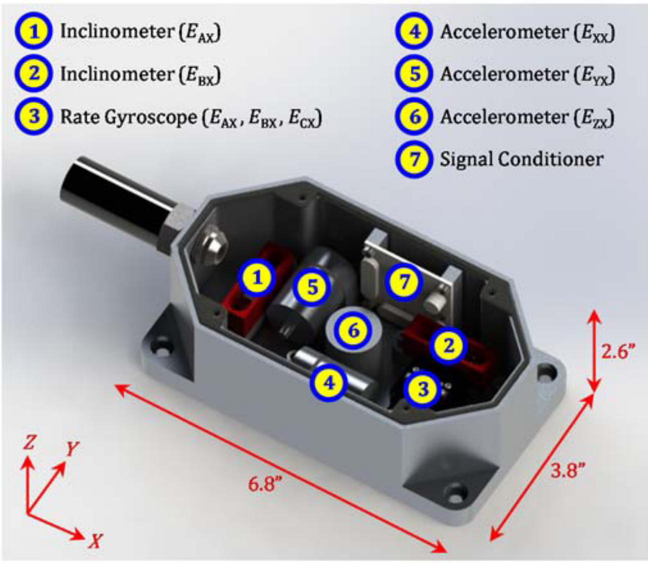

Figure 3. Rendered image of sensor box with sensors.

The sensor box top is not shown in Figure 3, so that the sensors can be seen. When the sensor box top is attached, a rubber seal between the box top and base ensure that the sensors are sealed for protection from machine tool environments (including fluids, metal chips, etc.).

3.2 Fixed-Cycle Test

For the fixed-cycle test, each of the axes is operated sequentially to move over its entire travel range at four constant speeds typical of linear axes, as seen in Table 3. Different axis speeds are used to account for the various sensor properties seen in Table 1, in order to minimize the measurement uncertainties of the estimated translational and angular errors. For example, the inclinometer requires a 'slow' speed due to its bandwidth of 2 Hz, while the accelerometer requires faster speeds to sense low spatial frequency motions due to its low cutoff frequency of 0.02 Hz.

Table 3. Fixed-cycle test speeds.

Speed Name	Speed (m/s)
Very Slow	0.004
Slow	0.02
Moderate	0.1
Fast	0.5

For research purposes, data may be collected for each axis while the carriage is moved in the positive or negative direction (2 directions) at each speed (4 speeds) for the desired number of runs (up to 50 runs). Data collection for multiple runs allows averaging for convergence purposes.

3.3 Data Processing

Once the fixed-cycle test data is collected, the data is integrated as needed. Rate gyroscope signals are integrated once to yield angular changes, and accelerometer signals are integrated twice to yield translational errors. Inclinometers may be used for direct measurement of angle from 0 Hz to about 2 Hz, as seen in Table 1. Then, the data is filtered and processed to yield the error components.

In order to estimate straightness errors, the 'data fusion' process shown in Figure 4 is based on the fact that signals generated by the same geometric errors can be decomposed into various frequency components via filtering and then added together to yield the original errors. Each filtered sensor signal yields a portion of the same geometric error over different neighboring spatial frequency ranges. Because these frequency ranges border each other, the error components add together to result in the originating geometric errors with wavelengths down to 0.1 mm. Also, the sensors must have relatively low noise in order to minimize drift, especially for the straightness errors based on double integration.

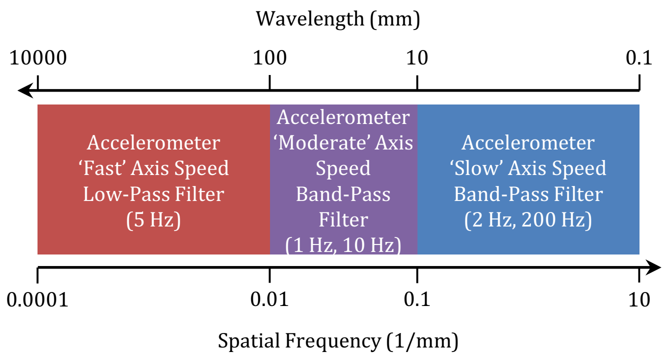

Figure 4. Fixed-cycle test data analysis for straightness errors.

Figure 5 shows the process to simulate the method in Figure 4 for the estimation of straightness error motions. As seen in Figure 5, a random straightness error is initially created with a maximum magnitude of 20 µm (see Table 2) and spatial frequency components with wavelengths as small as 40 µm. Next, the straightness error is measured by an accelerometer moving along the axis (1-meter long) at various speeds ('Slow', 'Moderate', and 'Fast' speeds; see Table 3). Thus, the same straightness is transformed in time to simulate measurement at each speed. The three acceleration signals are then filtered and sensor noise is added to each signal according to the accelerometer specifications. Analog output noise due to the data acquisition (DAQ) system is then added to the simulated signal and each of the three signals is then digitized and filtered based on the process bandwidths seen in Figure 4. The filtered signals are then integrated twice to yield three component displacements. These components are added together, with the resultant linear slope and bias removed, to yield the estimated straightness error. For 100 simulations with different randomly-generated straightness errors (the 'reference' errors), the difference between the reference and estimated straightness errors was within ± 5.6 µm, and the RMS of the difference over the entire axis travel was typically around 0.97 µm (Vogl, Weiss, & Donmez, 2015).

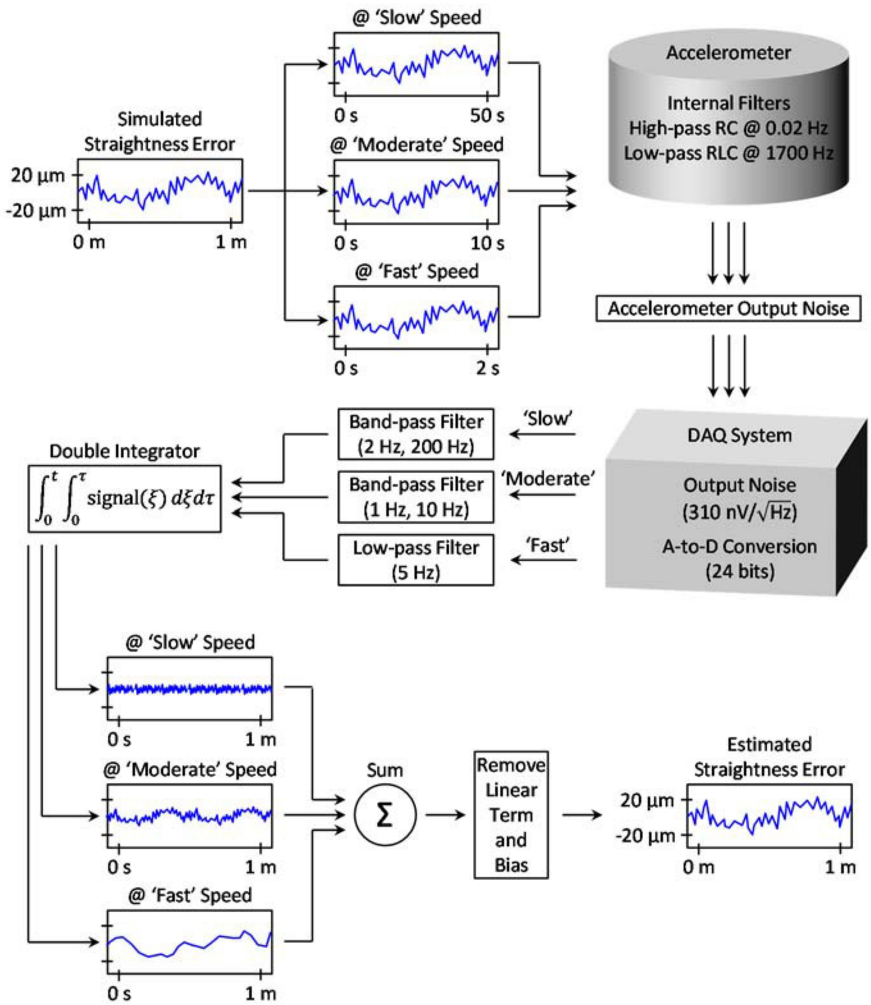

Figure 5. Simulated method of data acquisition and processing for estimation of straightness error motions.

For the estimation of angular errors, the various possible 'data fusion' processes are shown in Figure 6. Because both the inclinometer and rate gyroscope measure angular changes, the sensors could be used independently or dependently to estimate the angular error. Figure 6(a) shows how the inclinometer data can be used alone to determine angular errors with wavelengths above 2 mm (= 0.004 m/s / 2 Hz). However, such a process is only available for estimation of E_{AX} and E_{BX}, because no inclinometer exists for the Z-axis (for E_{CX}), as seen in Figure 3. In contrast, Figure 6(b) shows how the rate gyroscope data can be used to determine angular errors with wavelengths as low as 1 mm. This process is available for all three axes, because a rate gyroscope exists for every axis. Finally, Figure 6(c) shows how both the inclinometer and rate gyroscope data can be combined to yield the angular errors for the two axes with available inclinometer data.

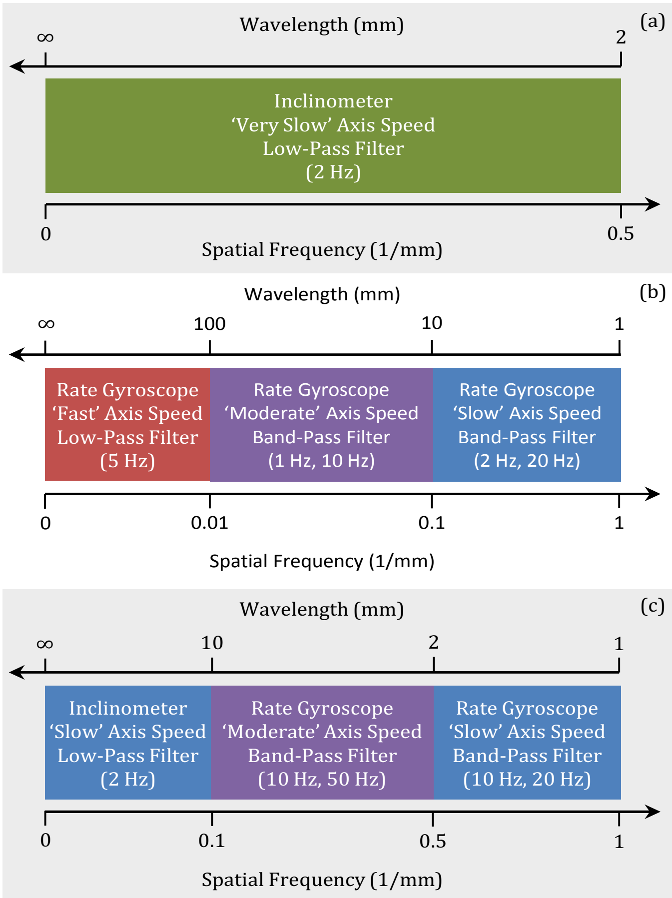

Figure 6. Possible data analysis schemes to estimate angular errors via use of (a) inclinometer data, (b) rate gyroscope data, or (c) both inclinometer and rate gyroscope data.

4 Implementation of Sensor-Based Method

The new sensor-based methodology for diagnostics of machine tool linear axes must be tested, verified, and validated experimentally. This section outlines the means for testing the accuracy of the sensor-based method for the detection of straightness and angular errors.

4.1 Linear Axis Testbed

A linear axis testbed was designed for testing the sensor-based method. As seen in Figure 7, the testbed is composed of a linear slide with a travel length of about 0.32 m. Sensor boxes move with the carriage: the sensor box for the new method and other boxes for a commercial laser-based system. The laser head contains a laser and interferometer, while the laser sensor boxes contain a retroreflector for displacement measurement, an electronic level for roll measurement, and sensor optics for pitch, yaw, and straightness measurements. The laser sensor boxes achieve a straightness error uncertainty of ±0.7 µm and an angular error uncertainty of ±3.0 µrad for 300 mm of travel. Due to its accuracy and precision, the laser-based system is used for validation and verification of the sensor-based method results. The linear slide is driven by a direct current (DC) motor with a rotary encoder attached to the motor shaft for motion control. The rotary encoder detects rotation with an accuracy corresponding to about ±0.7 µm in linear position, which is much smaller than the 0.1 mm resolution of the method (see Figure 4).

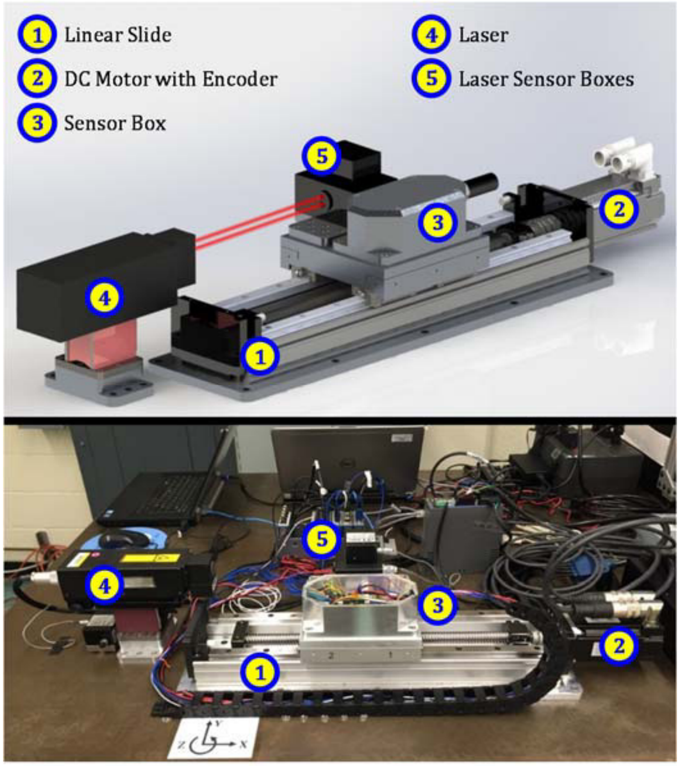

Figure 7. Rendered image and picture of linear axis testbed.

4.2 Data Collection

All data is collected with constant sampling rates while the carriage is controlled to move at a relatively constant speed from one end of the linear slide to the other end. Simultaneous data collection and motor control was enabled primarily via field-programmable gate array (FPGA), in which software was deployed to the instrumentation to allow real-time communication with the laptop during data collection. Table 4 shows the utilized sampling rates, which capture data within the needed filter bandwidths (as high as 200 Hz) seen in Figure 4. The position is not sampled at a constant data rate, but since each data point is uniquely timestamped, the non-constant sampling rate is acceptable.

Table 4. Sampling rates.

Sensor	Sampling Rate (Hz)
Position via Motor Encoder	72.4*
Inclinometer	100
Rate Gyroscope	995.7
Accelerometer	3200

* average sampling rate

As the first step towards verification and validation (V&V) of the sensor-based method, data was collected for the nominal state of the linear axis testbed. Sensor box data was collected for 50 runs during motion in each direction (positive or negative) at each of the 4 speeds, yielding 400 datasets. In contrast, the laser-based data was collected statically at locations with an interval of 0.25 mm. Furthermore, data was collected for each direction (positive or negative) approaching the static locations.

4.3 Angular Errors

Figure 8 shows the angular errors for a typical dataset processed according to Figure 6.

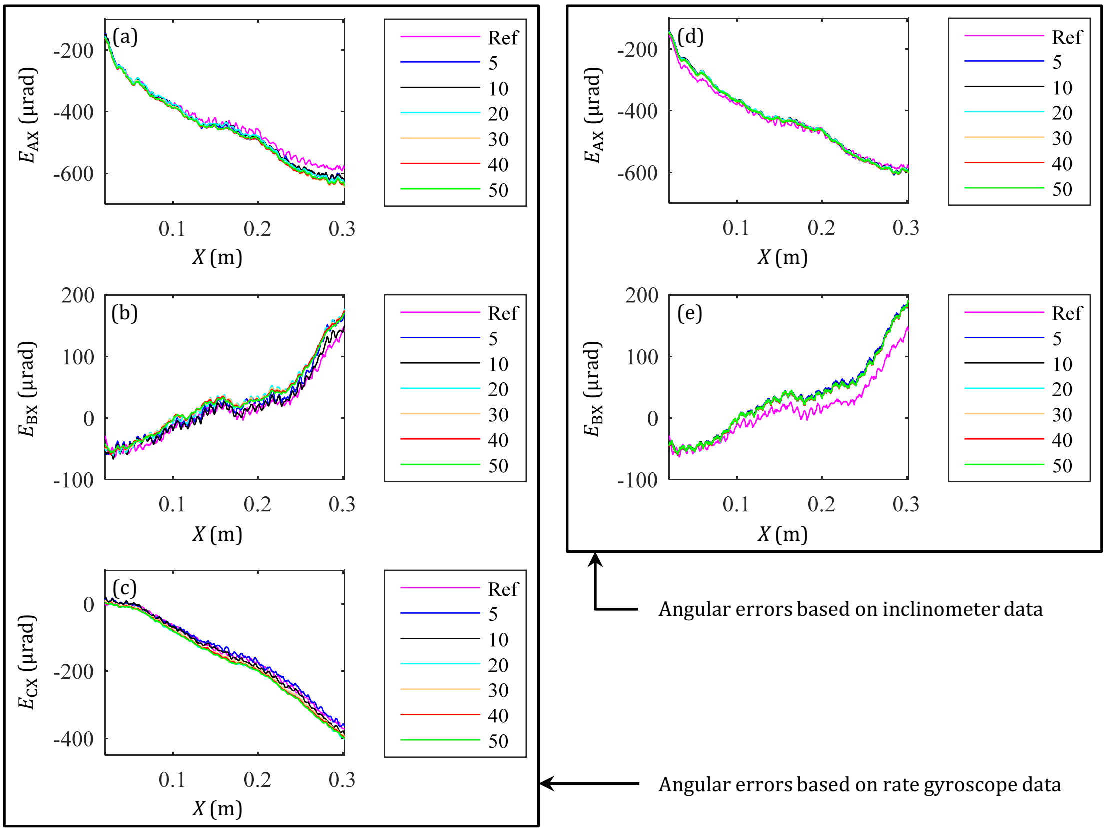

Figure 8. (a-c) Angular errors based on rate gyroscope data according to Figure 6(b), and (d-e) angular errors based on inclinometer data according to Figure 6(a), for various runs for averaging (5 to 50).

As seen in Figure 8, the angular errors converge as the number of runs used for averaging increases from 5 to 50. The angular errors in Figure 8(a-b), based on rate gyroscope data, converge slower with increasing number of runs for averaging compared to the angular errors in Figure 8(d-e), based on inclinometer data. This result is due to the effective larger angular noise of the rate gyroscope compared to the inclinometer (see Table 1). The net result is that the angular errors for 40 runs used for averaging are within ±4 μrad of the errors for 50 runs used for averaging. The uncertainties for these errors have not yet been established, but must be within ±6 μrad such that a TUR of at least 4:1 is possible based on the tolerance of 15 μrad seen in Table 2.

Despite the convergence, there are differences of up to about 40 μrad between the reference-based, gyroscope-based, and inclinometer-based angular errors in Figure 8. If these differences were based on uncertainties alone, then the TUR would be less than 4:1. In contrast, these differences are mainly physical: the converged angular errors for the three types (reference-, gyroscope-, or inclinometer-based) are physically different because each of the three data types were collected at different thermal states. Specifically, 50 runs of inclinometer data was collected at 'very slow' speed, and the rate gyroscope data was collected later in time for 'slow' to 'fast' speeds, per Table 3. As the motor moves the carriage forward and reverse at increasing speed, the linear stage undergoes thermal changes, especially in roll (E_{AX}), causing the main differences among the curves in Figure 8(a) and Figure 8(d). Once the system has equilibrated again, the laser-based data is collected statically and at its own unique thermal state. Other reasons for the discrepancies between the reference-based, gyroscope-based, and inclinometer-based angular errors are the various sources of uncertainty, including sensor misalignment, calibration, and nonlinearity, as well as modal vibrations that could influence the signals.

5 Conclusion

Manufacturers need quick and automated methods for diagnosis of machine tool linear axes with minimal disruptions to production. Towards this end, a new sensor-based methodology for diagnostics of machine tool linear axes was developed. The multi-sensor-based method uses data from inclinometers, accelerometers, and rate gyroscopes to identify changes in linear and angular errors due to axis degradation. This method began to be verified and validated via a linear axis testbed, which contains a linear axis and a reference laser-based system for measurement of the axis geometric performance. Comparison of the sensor-based results and the laser-based results shows that the sensor-based method is capable of detecting micrometer-level and microradian-level degradation of linear axes.

However, further testing is needed to verify that the sensor-based method is capable of achieving test uncertainty ratios (TURs) of at least 4:1 for both translational- and angular-related degradation. Once the method is verified for diagnostics of linear axes, further tests may show the value of certain metrics for prognostic purposes to estimate the remaining useful life (RUL) of linear axes performance. If the data collection and analysis are integrated within a machine controller, the process may appear to be seamless for the optimization of maintenance.

Acknowledgements

The authors thank the Fabrication Technology Group (NIST) for their outstanding contributions with the experimental setup. This work was also served by invaluable discussions with Brian Weiss (NIST) and Andreas Archenti (KTH Royal Institute of Technology, Sweden).

References

Altintas, Y., Verl, A., Brecher, C., Uriarte, L., & Pritschow, G. (2011). Machine tool feed drives. *CIRP Annals - Manufacturing Technology, 60*(2), 779-796. doi:http://dx.doi.org/10.1016/j.cirp.2011.05.010

Biehl, S., Staufenbiel, S., Recknagel, S., Denkena, B., & Bertram, O. (2012, June 27-29, 2012). *Thin Film Sensors for Condition Monitoring in Ball Screw Drives.* Paper presented at the 1st Joint International Symposium on System-Integrated Intelligence 2012: New Challenges for Product and Production Engineering, Hannover, Germany.

Ehrmann, C., & Herder, S. (2013). *Integrated diagnostic and preload control for ball screw drives by means of self-sensing actuators.* Paper presented at the 2013 WGP Congress, July 22, 2013 - July 23, 2013, Erlangen, Germany.

Feng, G.-H., & Pan, Y.-L. (2012). Investigation of ball screw preload variation based on dynamic modeling of a preload adjustable feed-drive system and spectrum analysis of ball-nuts sensed vibration signals. *International Journal of Machine Tools and Manufacture, 52*(1), 85-96. doi:10.1016/j.ijmachtools.2011.09.008

Garinei, A., & Marsili, R. (2012). A new diagnostic technique for ball screw actuators. *Measurement: Journal of the International Measurement Confederation, 45*(5), 819-828. doi:10.1016/j.measurement.2012.02.023

Huang, B., Gao, H., Xu, M., Wu, X., Zhao, M., & Guo, L. (2010, August 10-12, 2010). *Life prediction of CNC linear rolling guide based on DFNN performance degradation model.* Paper presented at the 2010 7th International Conference on Fuzzy Systems and Knowledge Discovery, FSKD 2010, Yantai, Shandong, China.

International Organization for Standardization. (2001). ISO 10791-2 - Test conditions for machining centres − Part 2: Geometric tests for machines with vertical spindle or universal heads with vertical primary rotary axis (vertical Z-axis).

International Organization for Standardization. (2012). ISO 230-1 - Test code for machine tools − Part 1: Geometric accuracy of machines operating under no-load or quasi-static conditions.

Khan, A. W., & Chen, W. (2009, November 16-19, 2008). *Calibration of CNC milling machine by direct method.* Paper presented at the 2008 International Conference on Optical Instruments and Technology: Optoelectronic Measurement Technology and Applications, Beijing, China.

Li, Y., Wang, X., Lin, J., & Shi, S. (2014). A Wavelet Bicoherence-Based Quadratic Nonlinearity Feature for Translational Axis Condition Monitoring. *Sensors, 14*(2), 2071-2088.

Liao, L., & Lee, J. (2009). A novel method for machine performance degradation assessment based on fixed cycle features test. *Journal of Sound and Vibration, 326*(3–5), 894-908. doi:10.1016/j.jsv.2009.05.005

Liao, L., & Pavel, R. (2012). *Machine tool feed axis health monitoring using plug-and-prognose technology.* Paper presented at the Proceedings of the 2012 Conference of the Society for Machinery Failure Prevention Technology.

Möhring, H.-C., & Bertram, O. (2012). Integrated autonomous monitoring of ball screw drives. *CIRP Annals - Manufacturing Technology, 61*(1), 355-358. doi:http://dx.doi.org/10.1016/j.cirp.2012.03.138

Ouafi, A. E., & Barka, N. (2013, March 13-14, 2013). *Accuracy enhancement of CNC multi-axis machine tools through an on-line error identification and compensation strategy.* Paper presented at the 2013 3rd International Conference on Advanced Measurement and Test, AMT 2013, Xiamen, China.

Plapper, V., & Weck, M. (2001, May 21-26, 2001). *Sensorless machine tool condition monitoring based on open NCs.* Paper presented at the 2001 IEEE International Conference on Robotics and Automation, Seoul, Korea, Republic of.

Shi, R., Guo, Z., Song, Z., & Yan, J. (2012, August 11-13, 2012). *Resarch of mechanical components' performance degradation based on dynamic fuzzy neural network.* Paper presented at the 2012 International Conference on Computer Science and Service System, CSSS 2012, Nanjing, China.

Uhlmann, E., Geisert, C., & Hohwieler, E. (2008). Monitoring of slowly progressing deterioration of computer numerical control machine axes. *Proceedings of the Institution of Mechanical Engineers, Part B: Journal of Engineering Manufacture, 222*(10), 1213-1219.

Verl, A., Heisel, U., Walther, M., & Maier, D. (2009). Sensorless automated condition monitoring for the control of the predictive maintenance of machine tools. *CIRP Annals - Manufacturing Technology, 58*(1), 375-378.

Vogl, G. W., Weiss, B. A., & Donmez, M. A. (2015). *A Sensor-based Method for Diagnostics of Machine Too Linear Axes*. Paper presented at the Annual Conference of the Prognostics and Health Management Society 2015, Coronado, CA.

Zhou, Y., Mei, X., Zhang, Y., Jiang, G., & Sun, N. (2009, May 25-27, 2009). *Current-based feed axis condition monitoring and fault diagnosis.* Paper presented at the 2009 4th IEEE Conference on Industrial Electronics and Applications, ICIEA 2009, Xi'an, China.

Zhou, Y., Tao, T., Mei, X., Jiang, G., & Sun, N. (2011). *Feed-axis gearbox condition monitoring using built-in position sensors and EEMD method*, Kidlington, Oxfordshire OX5 1GB, United Kingdom.

Zhou, Y., Xu, H., Liu, J., & Zhang, Y. (2014, August 3-6, 2014). *On-line backlash-based feed-Axis wear condition monitoring technology.* Paper presented at the 11th IEEE International Conference on Mechatronics and Automation, IEEE ICMA 2014, Tianjin, China.